International Journal of Nanomedicine

Dovepress
open access to scientific and medical research

Open Access Full Text Article

ORIGINAL RESEARCH

Pseudoephedrine Nanoparticles Alleviate Adriamycin-Induced Reproductive Toxicity Through the GnRhR Signaling Pathway

Yang Fu[1,2], Peipei Yuan[1,2], Yajuan Zheng[1], Yaxin Wei[1], Liyuan Gao[1], Yuan Ruan[1], Yi Chen[1], Panying Li[1], Weisheng Feng[1,2], Xiaoke Zheng[1,2]

[1]Department of Pharmacy, Henan University of Chinese Medicine, Zhengzhou, 450046, People's Republic of China; [2]The Engineering and Technology Center for Chinese Medicine Development of Henan Province, Zhengzhou, 450046, People's Republic of China

Correspondence: Xiaoke Zheng; Weisheng Feng, Department of Pharmacy, Henan University of Chinese Medicine, Zhengzhou, 450046, People's Republic of China, Email zhengxk.2006@163.com; fwsh@hactcm.edu.cn

Purpose: Pseudoephedrine (PSE) has rapid absorption and metabolism, which limits its pharmacologic actions. We postulated that pseudoephedrine nanoparticles (PSE-NPs) with high bioavailability could overcome this limitation. The defensive function of PSE-NPs nanoparticles against adriamycin-induced reproductive toxicity in mice was studied.

Methods: We encapsulated PSE in polylactide-polyglycolide nanoparticles (PLGA-NPs) and verified their protective activity against testicular injury in vivo and in vitro.

Results: We report a promising delivery system that loads PSE into PLGA-NPs and finally assembles it into a nanocomposite particle. In vitro, PSE-NPs reduced the adriamycin-induced apoptosis of GC-1 cells significantly, improved mitochondrial energy metabolism and promoted expression of the proteins related to the gonadotropin-releasing hormone (GnRh) receptor signaling pathway. In vivo, evaluation of sperm indices and histology showed that adriamycin could induce testicular toxicity. PSE-NPs significantly increased the sperm motility of mice, reduced the percent apoptosis and oxidative stress of testes, increased serum levels of GnRh, activated the GnRhR signaling pathway in testes and promoted expression of meiosis-related factors.

Conclusion: In view of their safety and efficiency, these PSE-NPs have potential applications in alleviating adriamycin-induced reproductive toxicity.

Keywords: pseudoephedrine nanoparticles, adriamycin, reproductive toxicity, GnRhR signaling pathway, sperm meiosis

Introduction

Testicular dysfunction and male infertility are the main late outcomes of anti-cancer treatment during childhood cancer.[1] Several studies have shown that different anti-cancer treatments, including chemotherapy and radiotherapy, can disrupt spermatogenesis in the testes of adolescents and preadolescent.[2] Cytotoxic treatment is aimed at rapidly dividing cells. Therefore, after cancer treatment, sperm generation can be weakened or even inhibited.[3] With the worldwide increase in cancer incidence, the use of cytotoxic drugs is increasing.[4] Although these drugs have potent side-effects, their use has become the cornerstone of treating and reducing the burden of cancer complications.[5]

Adriamycin is first-line treatment for several types of cancer in adults and children (breast, ovary, bladder, thyroid gland, leukemia).[6] Several authors have reported the harmful effects of adriamycin on the gonadal epithelial cells of cells. It damages testicular function for a long time by inducing chromosome aberration of spermatogonia, inhibits DNA synthesis and, eventually, leads to testicular atrophy.[7] Therefore, studying preventive and therapeutic drugs for reproductive toxicity is important.

Pseudoephedrine (PSE) is a nasal decongestant to treat the common cold. Recently, PSE has been reported to treat ejaculation disorders.[8,9] However, studies on PSE in reducing reproductive toxicity have rarely been reported. We wondered if PSE can improve adriamycin-induced reproductive toxicity. The low bioavailability and high clearance

Received: 25 November 2021
Accepted: 11 March 2022
Published: 1 April 2022

Graphical Abstract

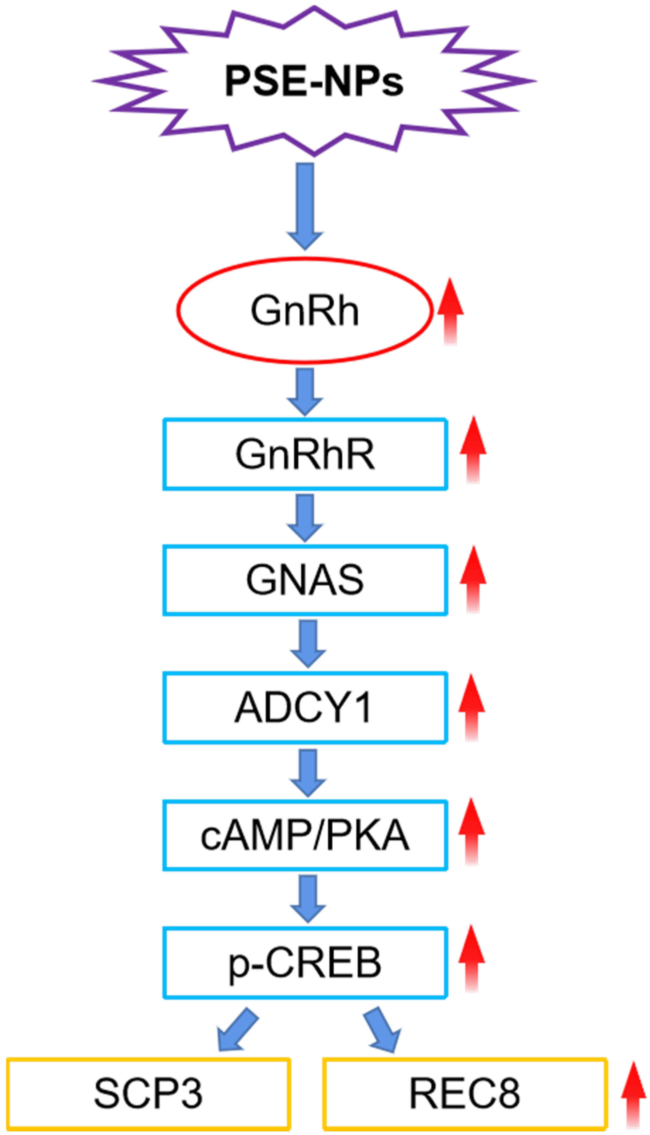

rate of PSE limit its application.[10] Therefore, we investigated the attenuation effect of pseudoephedrine nanoparticles (PSE-NPs) on adriamycin-induced reproductive toxicity in vitro and in vivo.

Materials and Methods

Chemicals

We obtained PSE from the National Institutes for Food And Drug Control (Beijing, China). Poly (ethylene glycol) methyl ether-poly(lactide-co-glycolide) (mPEG-PLGA; molecular weight (MW) = 18 kDa; LA/GA = 50:50; PEG MW = 2 kDa) was purchased from Jinan Daigang Biomaterials (Jinan, China). Poly (vinyl alcohol) (PVA; MW = 30–70 kDa; HD, 80%) and adriamycin were obtained from Sigma–Aldrich (Saint Louis, MO, USA). All other chemicals and reagents used were of analytical grade.

Preparation of PSE NPs

Briefly, the PSE aqueous solution (2 mg/mL) was mixed with PLGA dichloromethane (DCM) solution (50 mg/mL) with the volume ratio of 1:8 (v/v). After sonicating for 2 min, the mixture was dispersed into 1% PVA aqueous (containing 1% NaCl) with the volume ratio of 1:5 and sonicated for 2 min. The emulsion was stirred for 8h to obtain the stable double emulsion. DCM was volatilized to obtain a suspension of PSE-NPs. Large particles were removed by centrifugation at 2500× g for 2 min at room temperature, and then centrifuged at 2500× g for 5 min to obtain PSE-NPs. The precipitate was washed twice with deionized water, and unencapsulated drugs and impurities were removed. The precipitate was dispersed in 0.9% saline and stored at 4°C.

Characterization Studies of PSE NPs

Nano-ZS ZEN 3600 measured the polydispersion (PDI), mean size, and size distribution of PSE NPs using the dynamic light scattering technique. The tested samples were diluted 10 times for measurements. Each sample was measured three times in parallel. We examined the morphology of the PSE NPs by using SEM. We then viewed SEM images of PSE NPs by a Scanning Electron Microscope.[11]

Evaluation of PSE NPs Encapsulation Efficiency

We determined the nanoformulation encapsulation efficiency as the percent of PSE trapped in the nanoparticles. We then dissolved 25 mg of PSE NPs with 1 mL of 90% methanol, further subjected to sonication for 5 mins in order to cause disruption of the nanoparticles and release encapsulated PSE. The resulting solution at 10,000x g was centrifugated and we then gathered the supernatant. Supernatant absorption was read to quantify PSE at 425nm in a spectrophotometer (Thermo, MA, USA).[12]

Drug-Release Kinetics in vitro

Phosphate-buffered saline (PBS) supplemented with PSE-NPs was agitated in a constant-temperature shaker at 37°C in the dark. At 0.5, 1, 2, 4, 6, 9, 12, 24, 36, 48, 60 and 72 h after agitation, the solution was centrifuged at 2500× g to collect the supernatant, and the amount of PSE released in the supernatant was determined. Finally, the PSE concentration in the supernatant was determined using a ultraviolet spectrophotometer, after which the in vitro release profile was drawn.[13]

Cell Culture

A spermatogonia cell line from mice (GC-1) was obtained from American Type Culture Collection (Manassas, VA, USA). Cells were cultured in high-glucose Dulbecco's modified Eagle's medium containing 10% fetal bovine serum, 1% l-glutamine and a 1% penicillin–streptomycin mixture. Cells were set at 37°C in humidified air in an atmosphere of 5% carbon dioxide.

Determination of Apoptosis and Cell Viability

GC-1 cells were inoculated uniformly at $2×10^4$/mL in 96-well plates or $4×10^4$/mL in 6-well plates. The normal group underwent standard culture, whereas cells in the model group and other groups were damaged by 0.25 μM adriamycin for 24h. The PSE group was given PSE (0.5 μM). PSE-PLGA group was given PSE-NPs (PSE concentration 0.5μM). PLGA group was given the empty nanoparticles. Apoptosis was determined by staining (annexin V/propidium iodide) using the respective kit (BD Biosciences, Franklin Lakes, NJ, USA) and IDEAS 6.2 (Merck Millipore Biosciences, Waltham, MA, USA) was employed to calculate percent apoptosis. Cell viability was detected using the Cell Counting Kit (CCK)-8 assay (Abcam, Cambridge, UK) and absorbance was measured at 450 nm.

Determination of Mitochondrial Stress and Glycolysis Rate

GC-1 cells were plated onto XF-24 cell culture plates (American Seahorse Bioscience, North Billerica, MA, USA) and allowed to adhere overnight. Cells were divided into five groups. The normal group underwent standard culture, whereas cells in the M group and other groups were damaged by 0.25 μM adriamycin for 24h. The PSE group was given PSE (0.5 μM). PSE-PLGA group (PSE concentration 0.5μM), PLGA group was given the empty nanoparticles. After 24 h, the oxygen-consumption rate (OCR) and extracellular acidification rate (ECAR) were measured by a flux analyzer (XF-96, Hippocampus Bioscience, MA, USA) using a Seahorse XF Cell Mito Stress Test Kit (Agilent Technologies, Texas, USA) and glycolysis rate kit (Agilent Technologies, Texas, USA), respectively.[14]

Detection of the GnRhR Signaling Pathway in GC-1 Cells by a High-Connotation Imaging System

GC-1 cells were inoculated uniformly at 2×10^4/mL in 96-well plates (E190236X; PerkinElmer, Waltham, MA, USA). The normal group underwent standard culture, whereas cells in the M group and other groups were damaged by 0.25 μM adriamycin for 24h. The PSE group was given PSE (0.5 μM). PSE-PLGA group (PSE concentration 0.5μM), PLGA group was given the empty nanoparticles. After treatment with NPs, cells were washed with PBS, fixed with 4% paraformaldehyde for 20 min, permeabilized with 0.1% Triton for 20 min, and washed five times with PBS. Treated cells were blocked with 5% goat serum for 1.5 h at room temperature, incubated at 4°C overnight with primary antibody, then incubated with secondary antibody (Cy3 Goat Anti-Rabbit IgG; catalog number, AS007; ABclonal, Woburn, MA, USA) for 1 h at room temperature. Nuclei were counterstained with 4′,6-diamidino-2-phenylindole for 5 min. A high-connotation imaging system (Opera Phenix®; PerkinElmer) was used for scanning. The relative protein expression was normalized against control group using Harmony 4.8 (PerkinElmer).[15]

Establishment of an Animal Model

Fifty Kunming mice (25±2 g) (animal number: SCXK Beijing 2016–0006) were purchased from Beijing Victoria Experimental Animal Center (Beijing, China). The protocol for animal experiments was approved by the Animal Care and Use Committee of Henan University of Traditional Chinese Medicine (Zhengzhou, China). Experiments were carried out according to the guidelines and regulations of the Animal Care and Use Committee of the National Organization Engineering Center (Zhengzhou, China).

Mice were divided randomly into five groups of 10: control (Con), adriamycin-induced injury (Model), PSE, PLGA and PSE-PLGA. Mice in the CON group and Model group were administered normal saline (10 g/0.1 mL, i.v.). Mice in the PSE group and PSE-PLGA group were treated for 15 days before adriamycin-induced injury, once every 3 days. Each time, mice were injected (i.v.) with PSE (1.4 mg/kg), PSE-PLGAs (53.8 mg/kg) or PLGAs (53.8 mg/kg). NPs were prepared fresh every day based on the bodyweight of mice and were used immediately. Two days after the final administration, adriamycin (30 mg/kg, i.p.) was administered.[16,17] Two days later, all mice were killed. Sperm motility was detected, and tissues and blood were sampled. The tissues of mice in each group were stored at −80°C.

Histological Assessment

Testes taken for histopathological examination were placed in 10% buffered formalin solution and fixed for 48 hr. The samples were then subjected to routine procedures and embedded in paraffin blocks. The fixed testis samples were embedded in paraffin, 6 μm thick testes histological sections were cut and stained with hematoxylin-eosin to detect morphological alterations by a light microscope (Olympus BX53, Japan).[18]

Effects of PSE NPs on Sperm Parameters

The sperm motility (%), sperm density (million/mL), and the rates of dead sperm (%) were investigated in this study. The testis and epididymis were collected after mice were sacrificed, and immediately placed in the centrifuge tube with 37°C preheated physiological saline and cut up, put into 37°C water-bath, then incubated for 8 min; sperm motility and the rates of dead sperm was detected visually by sperm quality analyzer (Huazhong Medical Supplies Co., Ltd., Shijiazhuang, China) at 37°C. A total of 200 sperms per sample were evaluated. The percentage of sperms with forward and progressive activity was counted to assess sperm motility. Semen were collected, pretreated at 5% $NaHCO_3$ for 10 min, added as a suspension to the hemocytometer, and sperm count observed with light microscope (200×).[19]

Enzyme-Linked Immunosorbent Assay (ELISA)

Levels of GnRh, luteinizing hormone (LH), and testosterone in serum were measured using ELISA kits (Elabscience Biotechnology, Beijing, China) for GnRh (E-EL-0071c), LH (E-EL-M3053), and testosterone (E-EL-0155c), respectively. Levels of tumor necrosis factor (TNF)-α (E-EL-M0049c) and interleukin (IL)-1β (E-EL-M0037c) in testes were also measured, following the manufacturers' instructions.[20]

Measurement of Superoxide Dismutase (SOD) and Malondialdehyde (MDA) in Testicular Tissue

We determined the level of SOD and MDA in testicular tissue with the help of the respective test kits (Jiancheng, Nanjing, China). The steps were based on the manufacturers' protocol. All assays were performed in triplicate.[21]

Immunofluorescence

Levels of the testicular tissue-related proteins gonadotropin-releasing hormone receptor (GnRhR) and synaptonemal complex protein (SCP)3 were detected using antibodies against them (19950-1-AP and 23024-1-AP; Proteintech, Chicago, IL, USA). Fluorescent Cy3-coupled secondary antibodies were employed for detection.[22]

Western Blotting

The expression of GnRhR, GNAS, PKA, cAMP, p-CREB/CREB, SCP3, REC8, Bcl-2 and BAX was assayed by Western blotting. Testicular protein was extracted by a total protein extraction kit (BC3710; Beijing Solarbio Science & Technology, Beijing, China). Protein quantification was undertaken using a bicinchoninic acid kit (PC0020; Beijing Solarbio Science & Technology). A sodium dodecyl sulfate–polyacrylamide gel electrophoresis (SDS–PAGE) gel preparation kit (64136301; Bio-Rad Laboratories, Hercules, CA, USA) was used for gel preparation. Protein (50 μg) in each well was subjected to SDS–PAGE in 10% gels and transferred to 0.22 μm polyvinylidene difluoride (PVDF) membranes (Pall, Gelman Laboratory, USA). After membranes were blocked with 5% BSA in buffer for 2 h, primary antibodies against GnRhR (1:500 dilution; 19950-1-AP; Proteintech), guanine nucleotide binding protein (GNAS; 1:1000; ab283266; Abcam), protein kinase A (PKA; 1:1000; 12232-1-AP, Proteintech), phosphorylated-cyclic adenosine monophosphate (cAMP)-response element binding protein (p-CREB; 1:1000; 9198; Cell Signaling Technology, Danvers, MA, USA), CREB (1:1000; 12208-1-AP; Proteintech), SCP3 (small C-terminal domain phosphatase 3, 1:1000; 23024-1-AP; Proteintech), REC8 meiotic recombination protein (REC8; 1:1000; ab192241; Proteintech), cAMP (Cyclic Adenosine monophosphate, 1:1000; ab134901; Abcam), Caspase 3 (1:1000; ab32351, Abcam), Bax (BCL2-Associated X, 1:1000; 60267-1-Ig, Proteintech), Bcl-2 (B cell lymphoma-2, 1:1000; 60178-1-Ig, Proteintech) or β-Actin (1:5000; 66009-1-Ig; Proteintech) were added and incubation allowed to occur overnight at 4°C. After washing five times with Tris-buffered saline and Tween 20 (TBST), secondary antibody (1:20,000, C80911-11 and C80816-16, LI-COR) was added, and incubation allowed for 1 h at room temperature. Then, blots were washed thrice with PBS and Tween 20 (PBST) before Western blotting. The Odyssey two-color infrared fluorescence imaging system (Invitrogen, Carlsbad, CA, USA) was used for imaging. Western blot values were expressed after normalization to that of β-actin expression by Image Studio (LI-COR Biosciences, Lincoln, NE, USA).[15,22]

Real-Time RT-qPCR

According to manufacturer instructions, total RNA was extracted from testicular tissue or cells with a RNA extraction kit (Beijing Solarbio Science & Technology). The cDNA was synthesized from total RNA 5 mg using a reverse transcription kit (D7168M; Beijing Applygen Technologies, Beijing, China). Quantitative real-time RT-PCR was used to quantify the expression levels of different genes, using GAPDH mRNA as the normalization standard. The probes for genes, including GnRhR, LHR, AR, GNAS, ADCY1, PKA, DDX4, DAZ1, CYCLIN-1, STAR, SCP3, REC8, SMC1B, Miwi, TNF-α, IL-1β and Caspase 3 were designed by the manufacturer and purchased from were designed and synthesized by Beijing Genomics Institute (BGI). Amplification was performed under the following conditions: 1 min at 95°C; 5s at 95°C; 30s at 60°C with for 40 cycles, Melt Curve 65°C to 95°C. qRTPCR of mRNAs was performed using

SYBR™ qPCR Master Mix kit (Vazyme Biotech, Nanjing, China), and real-time PCR experiments were carried on the Thermo system (Quant studio 5). The sequences for the primers used in our study are listed in Table 1. Gene expression levels were calculated as a ratio to the expression of the reference gene, and data were analyzed using the $2^{-\Delta\Delta Ct}$ method.[21]

Statistical Analyses

Data are the mean ± SD. Data were analyzed with SPSS 19.0 (IBM, Armonk, NY, USA). Significant differences between groups were determined by one-way ANOVA. $P < 0.05$ was considered significant.

Results

Characterization of PSE-NPs

The maximum loading capacity and loading efficiency of PSE-NPs was 2.61±0.23% and 60.37±1.21%, respectively. The morphology and distribution of PSE-NPs was determined by scanning electron microscopy and photodynamics. PSE-NPs were revealed to be small and compact spheres (Figure 1A). The particle size distribution of PSE-NPs is primarily distributed between 295 and 615 nm, which is in line with the normal distribution characteristics.

The Polydispersity Index of PSE-NPs suspensions was <0.2. Figure 1 shows the quantity of the released drug against time for PSE-NPs. The average release rate of a drug up to 24 h was 71.52%, with rapid release of 34.28% in 5 h. Thereafter, the percentage release over 24 h increased steadily. These results indicated that PSE-NPs had good stability and monodispersity in distilled water.

Table 1 Primer Sequences

Target	Forward Primer (5′–3′)	Reverse Primer (5′–3′)	Accession Number	Product Size
GnRhR	TGCTCGGCCATCAACAACA	GGCAGTAGAGAGTAGGAAAAGGA	NM_001310653.1	114
LHR	CTCGCCCGACTATCTCTCAC	ACGACCTCATTAAGTCCCCTG	NM_001364898.1	77
AR	TGCCCGAATGCAAAGGTCTT	TTGGCGTAACCTCCCTTGAAA	NM_013476.4	94
GNAS	CAGAGCCTCCATTGGGGTC	GCTTCTCGCTCAACTGGGG	NM_001310085.1	141
ADCY1	TTGGCAAGTTCGATGAGTTAGC	GGCGTGATCCGTCTTAGGC	NM_009622.2	110
PKA	AGGGCAGGACATGGACATTG	CGCCTTATTGTAACCCTTGCTG	NM_001164199.1	80
DDX4	CGGATGATGCAGAGAGAGTACC	AATGATGGGCCTGAAAAAGAGTT	NM_001145885.1	157
DAZ1	ATACCTCCGGCTTATACAACTGT	GACTTCTTTTGCGGGCCATTT	NM_010021.5	128
CYCLIN-1	CAGTTTCCCCAATGCTGGTTG	CCTCTGCATACTCCGTTACGTTA	NM_001305221.1	99
STAR	GCCGGACCTCATGGAATTTGA	TCACTTCATGTGCAGAGATGATG	NM_009292.2	95
SCP3	AGCCAGTAACCAGAAAATTGAGC	CCACTGCTGCAACACATTCATA	NM_011517.2	106
REC8	GGTCATCACCTTACAGGAGGC	TCTGCGATCAGCAGTTCTAAGT	NM_001360390.1	105
SMC1B	CATGAGGGAAAACGTCAGCAG	TGACACAGATCAAGCAGTCTTC	NM_080470.1	98
Miwi	AGACCTCATTGGAAGGTGTCA	TGTTCCCCATTCCGAGTCTGA	NM_021311.3	108
TNF-α	CTGAACTTCGGGGTGATCGG	GGCTTGTCACTCGAATTTTGAGA	NM_013693.3	122
IL-1β	GAAATGCCACCTTTTGACAGTG	TGGATGCTCTCATCAGGACAG	NM_008361.4	116
Caspase 3	TGGTGATGAAGGGGTCATTTATG	TTCGGCTTTCCAGTCAGACTC	NM_009810.3	105
GAPDH	TGTGTCCGTCGTGGATCTGA	TTGCTGTTGAAGTCGCAGGAG	NM_008084.3	150

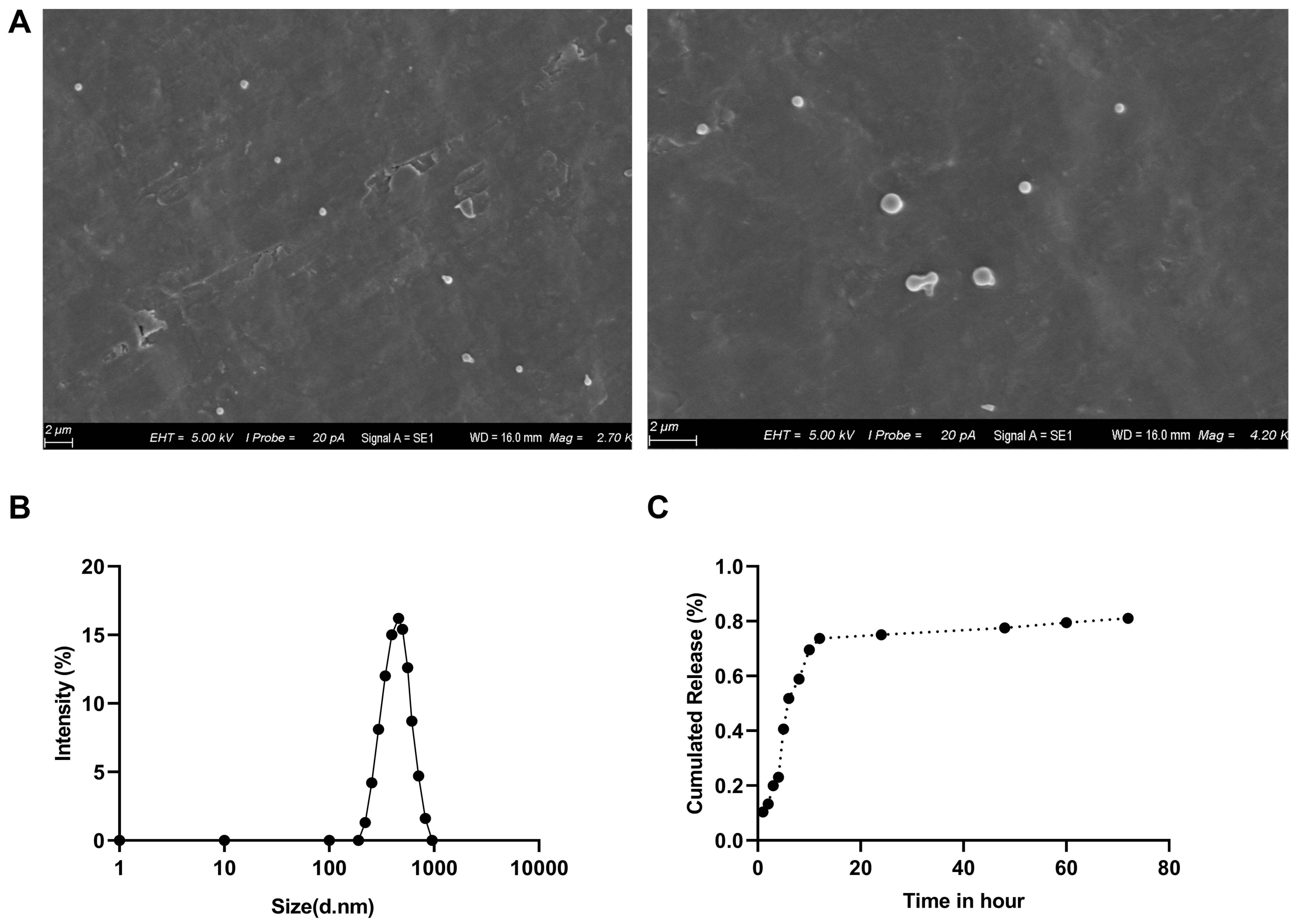

Figure 1 Characterization of PSE-NPs: (**A**) SEM micrographs of the PSE NPs. (**B**) Dynamic light scattering of pseudoephedrine nanoparticles (PSE-NPs) and (**C**) in vitro release of PSE-NPs.

Effect of PSE-NPs on the Survival and Percent Apoptosis of GC-1 Cells Damaged by Adriamycin

Adriamycin significantly increased the percentage of GC-1 cells that underwent apoptosis and reduced the percentage of cells that survived, whereas PSE-NPs significantly increased the percentage of GC-1 cells that survived and decreased percent apoptosis (Figure 2A and B). PSE and PSE-NPs could significantly reduce expression of the apoptosis-related proteins BAX and caspase 3, and increase expression of Bcl-2 (Figure 2C). When compared with free-PSE treated group, the effect of PSE-NPs was enhanced. These results confirmed that PSE-NPs can efficiently inhibit the apoptosis of GC-1 cells, the application of NPs significantly improved the effect.

Effect of PSE-NPs on Mitochondrial Energy Metabolism and Glycolysis Rate of GC-1 Cells Damaged by Adriamycin

To investigate how NPs rescue mitochondrial function, we measured the OCR and ECAR of GC-1 cells by analyzing extracellular flux. Compared with the CON group, the cellular metabolism of the Model group was lower (Figure 3). However, inhibition of the OCR was rescued by PSE-NPs treatment, including basal respiration, adenosine triphosphate (ATP) production, and maximal respiration. Adriamycin was shown to reduce basic glycolysis and compensatory glycolysis: PSE-NPs could increase both significantly. At the same concentration, the effect of PSE-NPs better than free-PSE treated group. Taken together, these results suggested that the application of PSE-NPs significantly increased the mitochondrial energy metabolism and glycolysis rate of GC-1 cells.

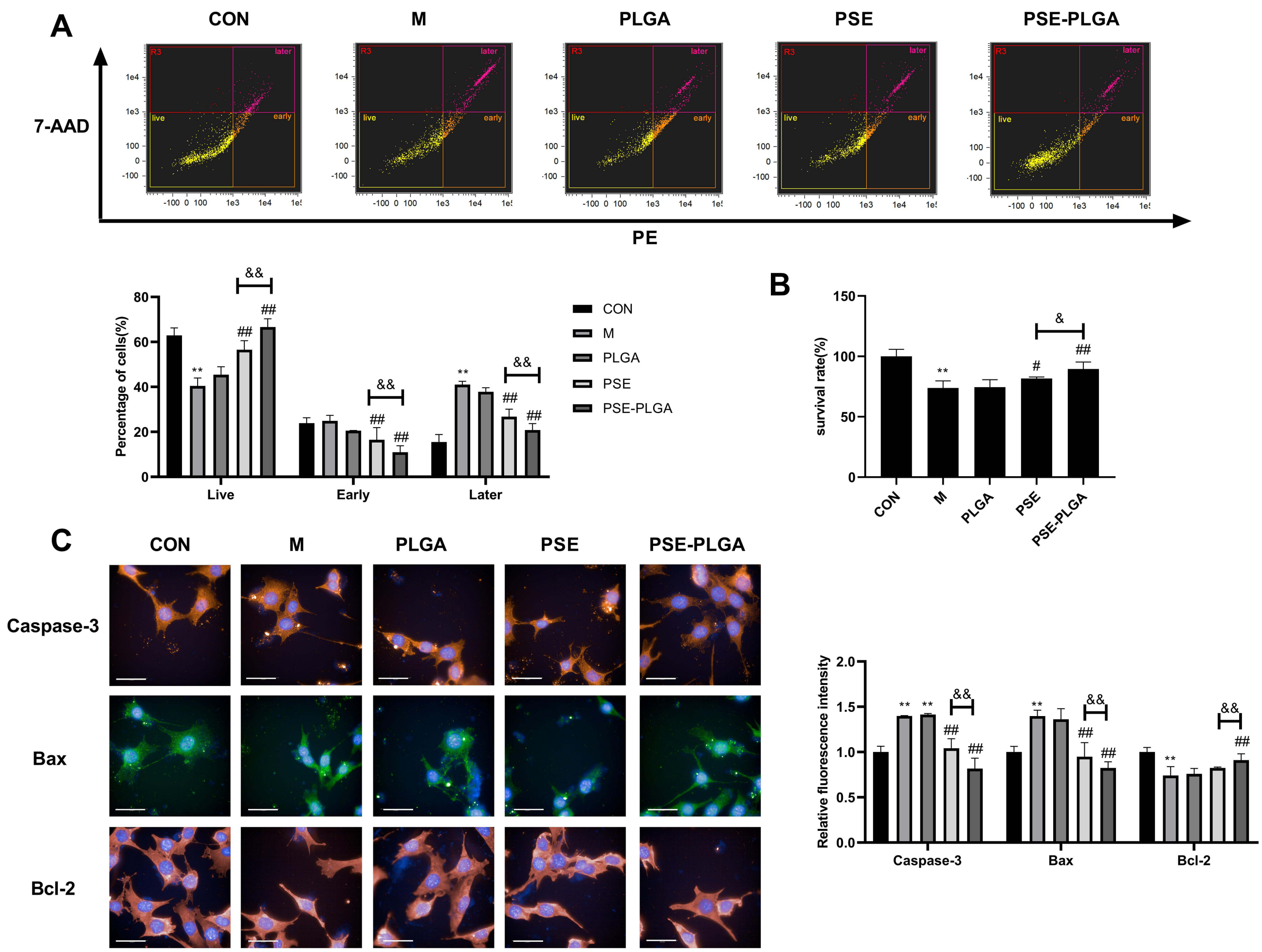

Figure 2 Effect of pseudoephedrine nanoparticles (PSE-NPs) on percent apoptosis of GC-1 cells and expression of apoptosis-related proteins: (**A** and **B**) Effect of PSE-NPs on percent apoptosis and survival of GC-1 cells in each group. (**C**) Effect of PSE-NPs on expression of apoptosis-related proteins of each group, scale bar 50 μm.
Notes: Data are the mean ± SD (n = 6). $^{**}P < 0.01$ vs the CON group. $^{\#}P < 0.05$ and $^{\#\#}P < 0.01$ vs the Model group. $^{\&}P < 0.05$ and $^{\&\&}P < 0.01$ vs the PSE group.
Abbreviations: CON, control group underwent standard culture; M, model group; PLGA, empty nanoparticles; PSE, 0.5μM pseudoephedrine; PSE-PLGA, 0.25 μM pseudoephedrine-loaded PLGA nanoparticles; Bax, BCL2-Associated X; Bcl-2, B cell lymphoma-2.

Effect of PSE-NPs on the GnRhR Signaling Pathway and Expression of Meiosis-Related Proteins SCP3 of GC-1 Cells Damaged by Adriamycin

The effect of PSE-NPs on the GnRhR signaling pathway of GC-1 cells damaged by adriamycin was detected by a high-connotation imaging system. Compared with the CON group, protein expression of the GnRhR signaling pathway and sperm meiosis (hereafter termed "meiosis")-related protein SCP3 in the Model group was decreased significantly, and that in the PSE group and PSE-NPs group increased significantly, and the effect of PSE-NPs was more robust than that observed in the PSE group (Figure 4).

Effects of PSE-NPs on Bodyweight, Testicular Indices, Testes Histology, and Sperm Motility of Adriamycin-Treated Mice

Deaths or abnormal clinical signs were not observed in mice of any group. There was no significant difference in bodyweight between the five groups (Table 2). The testicular structure and spermatogenic cells of mice in the CON group were normal. Mice in the Model group and PLGA group had cell shedding, and a decrease in the spermatogenic-cell layer. Compared with the Model group, the PSE group and PSE-PLGA group had significantly increased number of germ

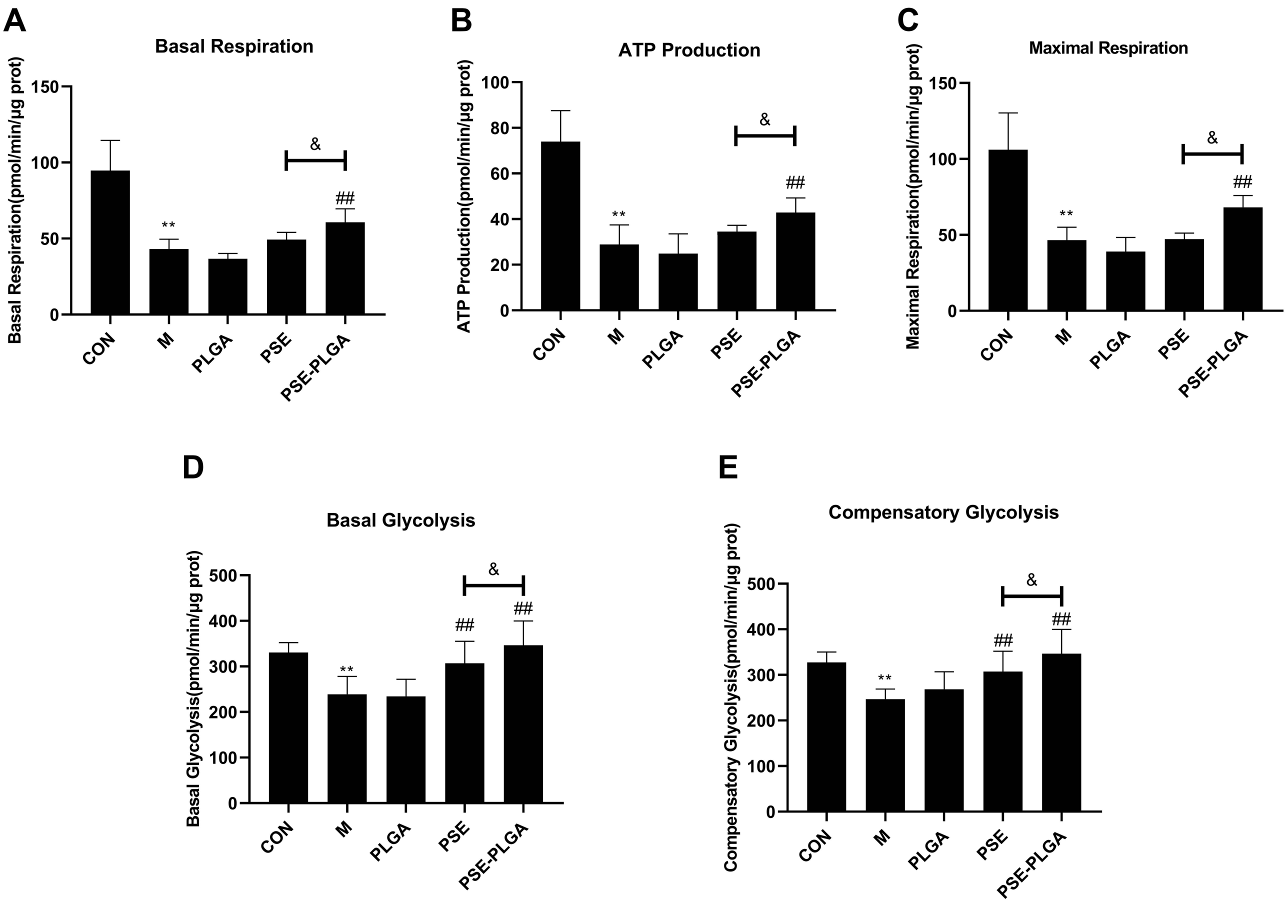

Figure 3 Effects of pseudoephedrine nanoparticles (PSE-NPs) on the mitochondrial functions and glycolysis rate of GC-1 cells: (**A**–**C**) Effects of PSE-NPs on basal respiration, ATP production, and maximal respiration in each group. (**D** and **E**) Effects of PSE-NPs on basal glycolysis and compensatory glycolysis in each group.
Notes: Data are the mean ± SD (n = 6). $^{**}P$ < 0.01 vs the CON group. $^{\#\#}P$ < 0.01 vs the Model group. $^{\&}P$ < 0.05 vs the PSE group.
Abbreviations: CON, control group underwent standard culture; M, model group; PLGA, empty nanoparticles; PSE, 0.5μM pseudoephedrine; PSE-PLGA, 0.25 μM pseudoephedrine-loaded PLGA nanoparticles.

cell layers and improved cell shedding (Figure 5). The effects of treatment on the Testes Index and Epididymis Index (Ratio of Testes weight or Epididymis weight to body weight) of mice are shown in Table 2. The Epididymis Index in the Model group decreased significantly, whereas the Epididymis Index in the PSE-NPs group increased significantly, compared with Model group. Compared with the CON group, the number of sperm and sperm motility in the Model group were decreased significantly, and the number of dead sperm was increased significantly; PSE-NPs could increase the number of sperm and sperm motility significantly, and reduce the number of dead sperm significantly, and the effect of PSE-NPs was more obvious than that free-PSE group.

Effect of PSE-NPs on Oxidative Stress

Lipid peroxidation was evaluated by measuring levels of SOD and MDA. Adriamycin treatment reduced the SOD level markedly but increased the level of MDA (P < 0.01) (Figure 6B and C). PSE-NPs could restore the SOD level and reduce the MDA level (P<0.01). Our findings suggested that PSE-NPs could reduce oxidative stress in adriamycin-treated mice.

Effect of PSE-NPs on Percent Apoptosis and Expression of Apoptosis-Related Proteins in the Testicular Cells of Adriamycin-Treated Mice

Apoptosis in testicular cells was detected by flow cytometry. Adriamycin increased the percent apoptosis of testicular cells significantly (P < 0.01), and PSE-NPs treatment could reduce the percentage of apoptotic cells significantly (P < 0.01) (Figure 6A). ADM increased the MDA level significantly and decreased the SOD level significantly, and PSE-NPs could

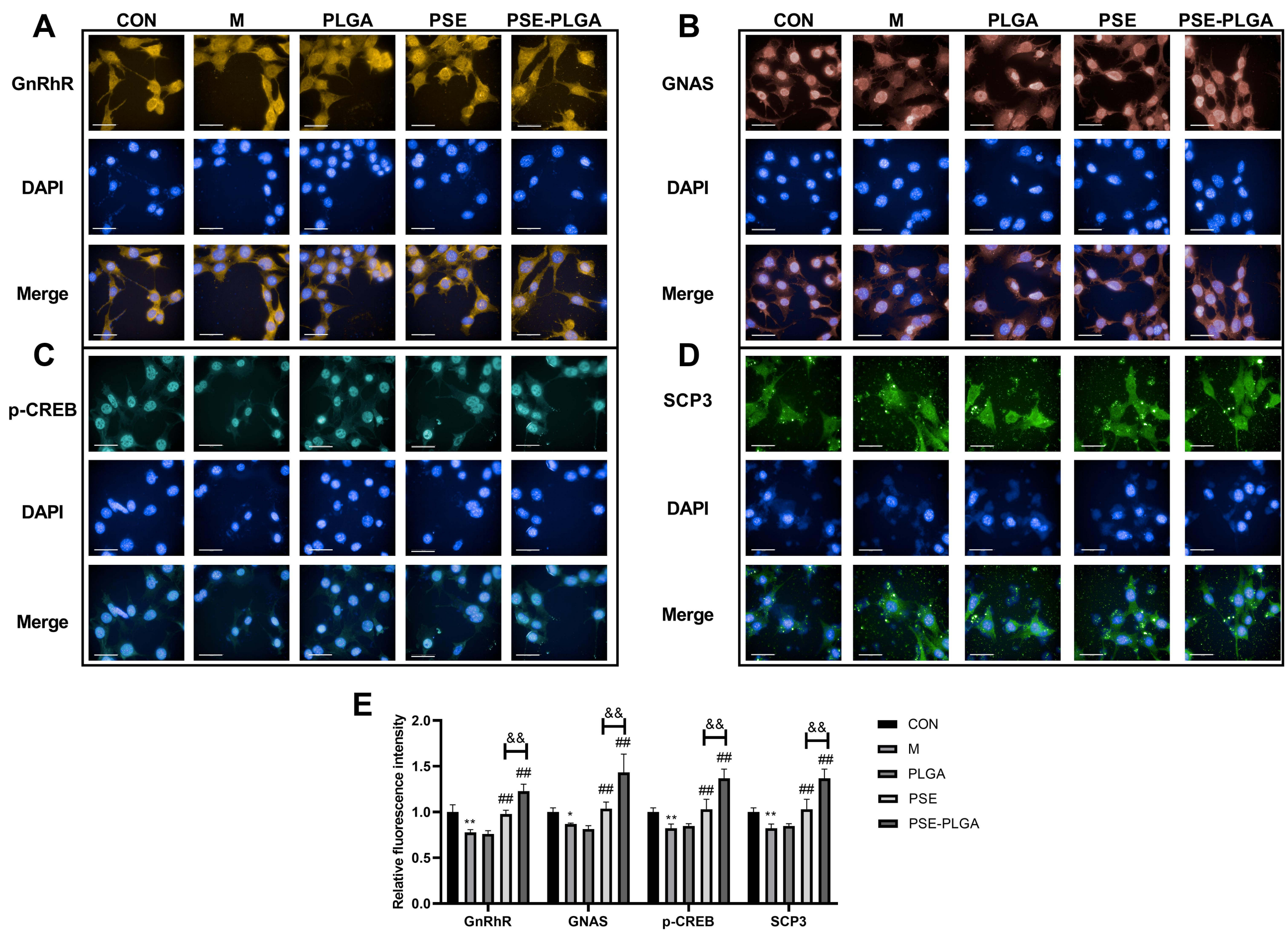

Figure 4 Effect of PSE-NPs on the GnRhR signaling pathway and expression of meiosis-related proteins SCP3 of GC-1 cells damaged by adriamycin: (**A**–**E**) Protein expression of GnRhR, GNAS, p-CREB and SCP3 in GC-1 cells, scale bar 50 μm.

Notes: Data are the mean ± SD (n = 6). *P < 0.05 and **P < 0.01 vs the CON group. ##P < 0.01 vs the Model group. &&P < 0.01 vs the PSE group.

Abbreviations: CON, control group underwent standard culture; M, model group; PLGA, empty nanoparticles; PSE, 0.5μM pseudoephedrine; PSE-PLGA, 0.25 μM pseudoephedrine-loaded PLGA nanoparticles; GnRhR, gonadotropin-releasing hormone receptor; CREB, cyclic adenosine monophosphate (cAMP)-response element binding protein; GNAS, guanine nucleotide binding protein; SCP3, small C-terminal domain phosphatase 3.

reverse these effects (P < 0.01) (Figure 6B and C). We measured expression of Bax and Bcl-2 by western blotting. Adriamycin increased Bax expression significantly and decreased Bcl-2 expression significantly (P < 0.01) but PSE-NPs could reverse these effects (P < 0.01) (Figure 6D). RT-qPCR revealed that adriamycin could upregulate mRNA expression of TNF-α, IL-1β and caspase-3 (P < 0.01), whereas PSE-NPs could inhibit their expression significantly (P < 0.01).

Effect of PSE-NPs on Sex-Hormone Levels in Mice Treated with Adriamycin

Testicular levels of testosterone are regulated in part by the levels of GnRh and LH. GnRh and LH are involved in the synthesis and regulation of testosterone in the testes. After intraperitoneal injection of adriamycin, compared with that in control group, the levels of GnRh, LH and testosterone in the serum of mice were decreased significantly (P < 0.01), and PSE-NPs treatment could increase the levels of GnRh, LH and testosterone significantly compared with that free-PSE group (P < 0.01 or P < 0.05).

Effects of PSE-NPs on the GnRhR Signaling Pathway and Meiosis-Related Indices in the Testes of Adriamycin-Treated Mice

We measured expression of GnRhR signaling pathway-related proteins in the testes of mice in each group by western blotting. Compared with control group, expression of GnRhR, GNAS, PKA, cAMP and p-CREB in the model group was

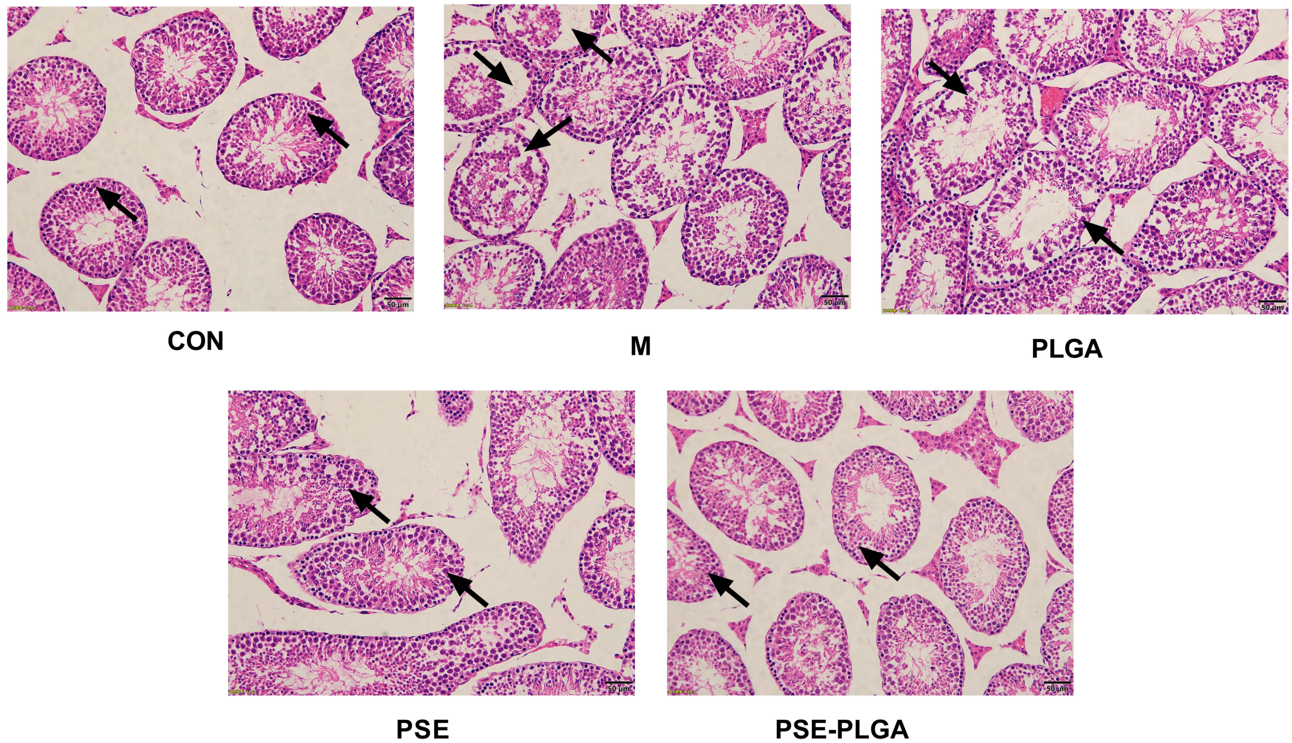

Figure 5 Effect of PSE-NPs on testicular histology in mice. The CON group showed a normal organizational structure. The Model group and PLGA group showed cell shedding and a decrease in the spermatogenic-cell layer. Compared with the Model group, the PSE group and PSE-PLGA group had significantly improved histology, and the PSE-PLGA group had the best effect. Black arrows mark showing spermatogenic cell layers.
Abbreviations: CON, Control group; M, Model group with 30 mg/kg adriamycin, i.p.; PSE, 1.4 mg/kg PSE, i.v.; PLGA, 53.8 mg/kg PLGAs, i.v.; PSE-PLGA, 53.8 mg/kg PSE-PLGAs, i.v.

decreased significantly. PSE-NPs treatment could increase expression of these proteins significantly. We used RT-qPCR to measure gene expression of GnRhR signaling pathway-related proteins. Expression of the genes for GnRhR, luteinizing hormone receptor (LHR), androgen receptor (AR), GNAS, PKA and adenylate cyclase 1 (ADCY1) in the Model group was reduced significantly compared with that in control group. PSE-NPs treatment could reverse these effects.

SCP3 and REC8 have key roles in meiosis. We measured protein and gene expression by western blotting and RT-qPCR. Expression of SCP3 and REC8 in the model group decreased significantly compared with that in control group and PSE-NPs treatment could increase expression of SCP3 and REC8 significantly. We also measured expression of the genes closely related to SCP3: deleted in azoospermia protein (Daz)1, DDX4, cyclin-1, StAR-related lipid transfer protein 8 (STAR), structural maintenance of chromosomes protein 1B (SMC1B) and murine piwi (Miwi). Expression of these genes in the model group decreased significantly compared with that in control group and PSE-NPs treatment could

Table 2 Effects of PSE-NPs on Bodyweight, Testicular Indices, and Sperm Motility in Mice Treated with Adriamycin

	CON	Model	PLGA	PSE	PSE-PLGA
Weight, g	36.5±2.0	35.0±2.9	35.0±2.3	35.5±2.1	35.3±1.5
Testes Index	6.60±0.36	4.59±0.43**	4.48±0.46	5.14±0.22	5.89±0.68$^{\#\#\&}$
Epididymis index	1.39±0.20	0.86±0.14**	0.68±0.09	1.22±0.07$^{\#}$	1.49±0.24$^{\#\#}$
Motility, %	69.4±7.6	20.4±7.3**	26.5±9.0	49.4±8.6$^{\#\#}$	62.2±10.3$^{\#\#\&\&}$
Density, ×10^6	190.0±40.6	88.3±27.2**	83.2±12.0	101.1±22.0	132.0±15.5$^{\#\#\&}$
Dead sperm, %	17.3±3.8	65.1±4.9**	59.9±8.8	43.6±14.1$^{\#\#}$	31.1±12.1$^{\#\#\&\&}$

Notes: Data are the mean ± SD (n = 8). ***P* < 0.01 vs the CON group. $^{\#}P$ < 0.05 and $^{\#\#}P$ < 0.01 vs the Model group. $^{\&}P$ < 0.05 and $^{\&\&}P$ < 0.01 vs the PSE group.

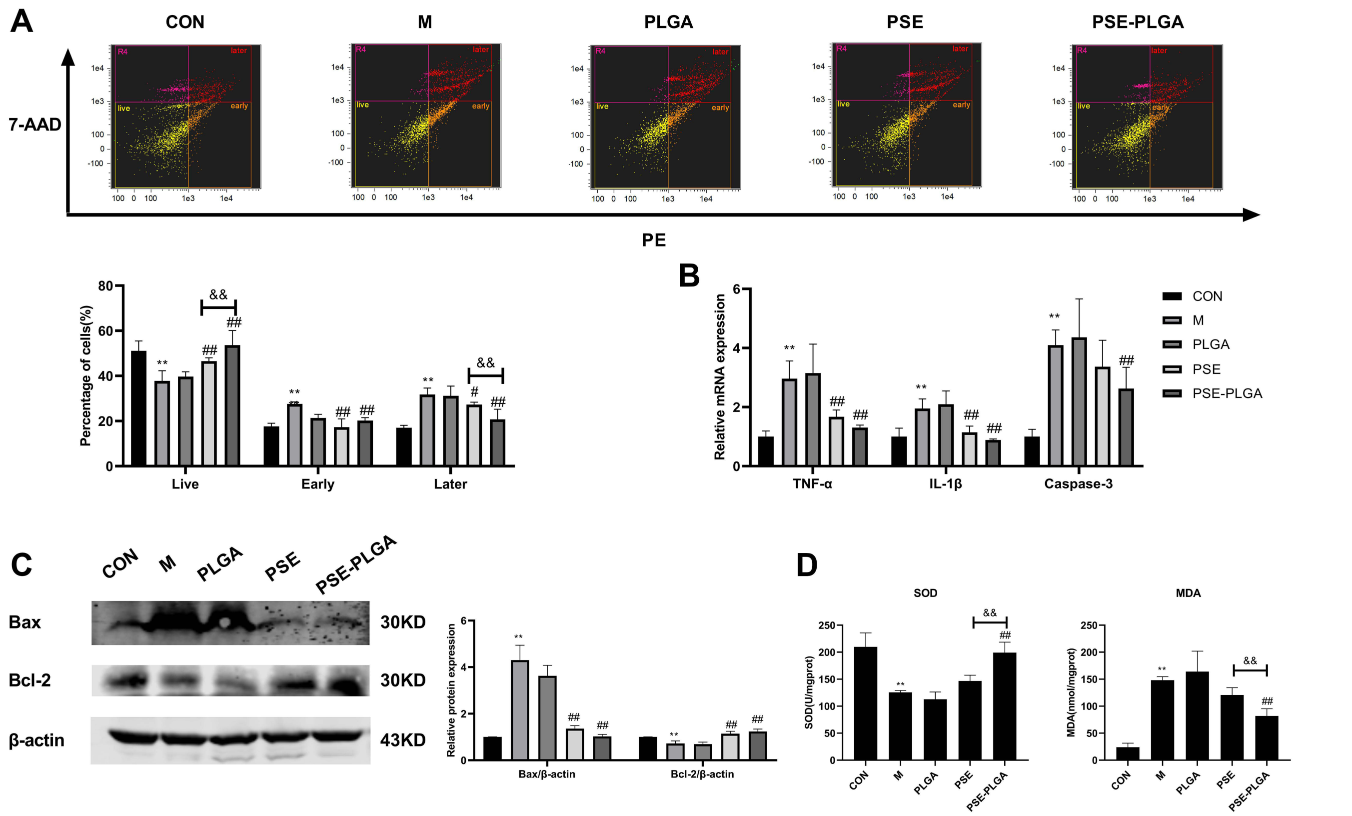

Figure 6 Effects of PSE-NPs on percent apoptosis, oxidative stress, and expression of apoptosis-related proteins in mouse testicular cells: (**A**) Percent apoptosis in the testicular tissue of mice in each group. (**B**) mRNA expression of IL-1β, caspase 3 and TNF-α in the testicular tissue of mice each group measured by RT-qPCR. (**C**) Protein expression of Bax and Bcl-2 in the testicular tissue of mice in each group measured by Western blotting. (**D**) Levels of SOD and MDA in the testicular tissue of mice in each group.

Notes: Data are the mean ± SD (n = 6). $^{**}P < 0.01$ vs the CON group. $^{\#}P < 0.05$ and $^{\#\#}P < 0.01$ vs the Model group. $^{\&\&}P < 0.01$ vs the PSE group.

Abbreviations: CON, Control group; M, Model group with 30 mg/kg adriamycin, i.p.; PSE, 1.4 mg/kg PSE, i.v.; PLGA, 53.8 mg/kg PLGAs, i.v.; PSE-PLGA, 53.8 mg/kg PSE-PLGAs, i.v.; 7-AAD, 7-amino-actinomycin D; PE, Phycoerythrin; TNF-α, tumor necrosis factor-α; IL-1β, interleukin-1β; Bax, BCL2-Associated X; Bcl-2, B cell lymphoma-2; SOD, Superoxide dismutase; MDA, Mobile device assistant.

increase expression significantly. Further, we detected GnRHR and SCP3 levels again by immunofluorescence, which was consistent with the results of WB and RT-qPCR (Figure 7).

Discussion

Adriamycin is used to treat a wide variety of cancer types. However, adriamycin treatment can lead to testicular injury.[23,24] Studies have shown that PSE can improve sperm motility[9,25] and NPs can help to promote repair of testicular tissue.[26,27] PSE is metabolized readily and has a short half-life in vivo,[10] so we constructed PSE-NPs. PLGA has good biocompatibility, safety and stability. It is a biodegradable polymer material. Its degradation products and metabolites are non-toxic and will not remain in the body.[28,29] Therefore, PLGA has been approved by the US Food and Drug Administration (FDA) as a pharmaceutical excipient. The PLGA controlled release system can maintain effective blood drug concentration, reduce the number of administrations, reduce the dosage, improve the curative effect and improve the body compliance.[30] Compared to other metallic materials, no reports of reproductive toxicity were found. However, ordinary nanoparticles are easily recognized by phagocytic cell lines and rapidly cleared in the human body. Polyethylene glycol (PEG) modified PLGA block copolymers are amphiphilic.[31] The outer layer of the nanoparticles is a hydrophilic PEG shell, which can escape the clearance of macrophages, which can further improve the efficacy of the loaded drug. Therefore, PEG-PLGA was selected for drug loading. The final nanoparticles with a diameter of about 396 nm, displayed a good PDI, encapsulation efficiency, and drug loading. The latter can be released slowly in vivo, which contributes to their efficacy.

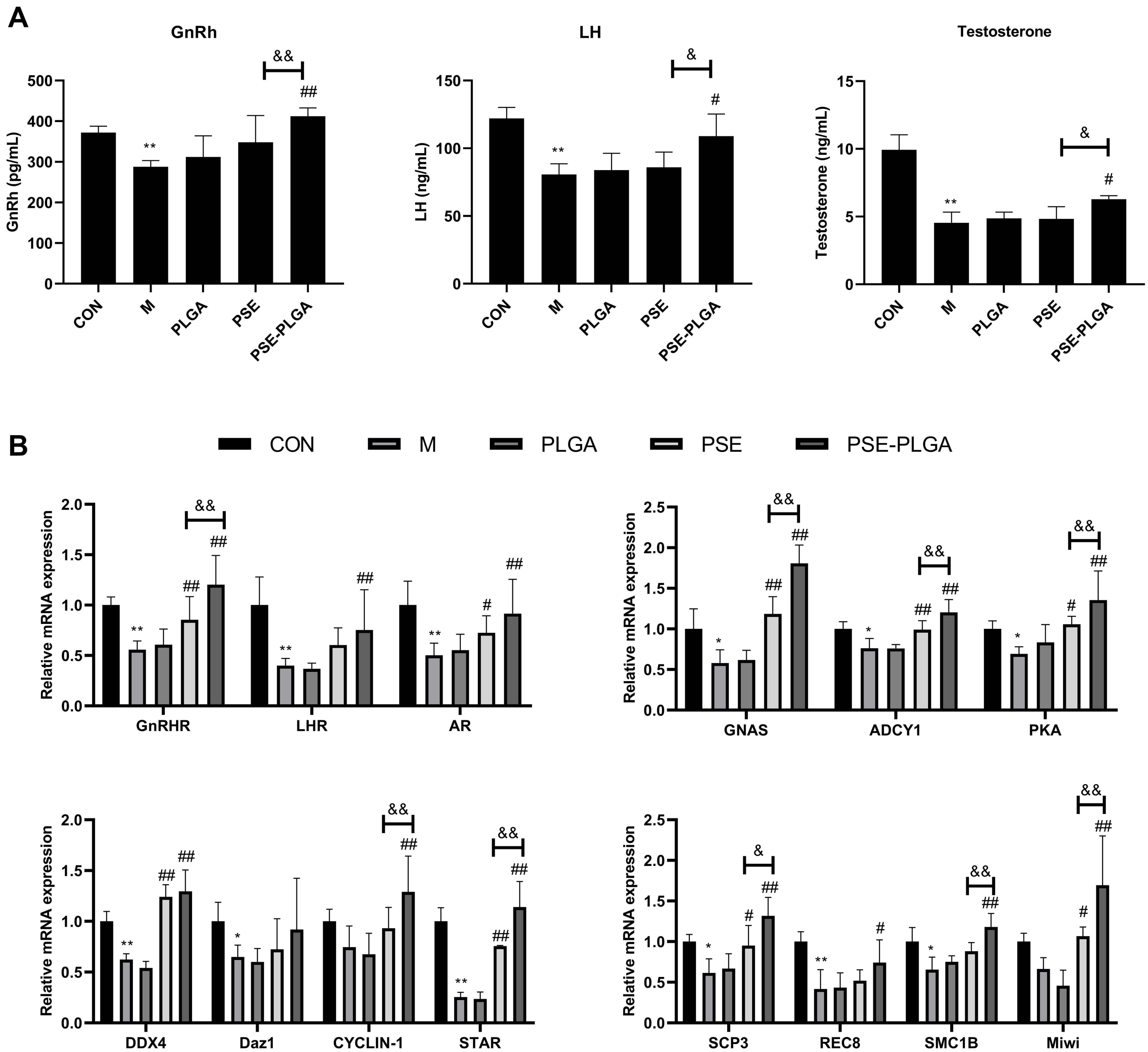

Figure 7 Continued.

BCl2 and Caspase family proteins play a key role in controlling apoptosis. Bcl2 is an inhibitor of apoptosis protein, Bax and Caspase 3 are pro-apoptotic proteins.[32,33] We evaluated the protective effect of PSE-NPs by detecting the apoptosis-related proteins Bax, Bcl-2 and Caspase 3. We showed that, in vitro, PSE-NPs could increase the survival of GC-1 cells significantly, reduce the percent apoptosis of GC-1 cells, regulate expression of Bax and Bcl-2, and significantly reduce the level of caspase 3. In recent years, scholars have shown that sperm generation is closely related to mitochondrial energy metabolism.[34] The efficiency of glycolysis and maintenance of spermatogenesis are very important.[35] Increasing glycolysis cascades and ATP production help to improve the damage to testicular cells.[36] Hence, we measured the level of mitochondrial energy metabolism: PSE-NPs could significantly increase the level of mitochondrial energy metabolism. In the present study, we used a high-connotation imaging system for detection of expression of proteins related to the GnRhR signaling pathway and meiosis. We found that PSE-NPs could significantly activate expression of GnRhR signaling pathway-related proteins and increase expression of the meiosis-related protein SCP3. These results confirmed that PSE can efficiently inhibit the apoptosis and activate GnRhR signaling pathway, the

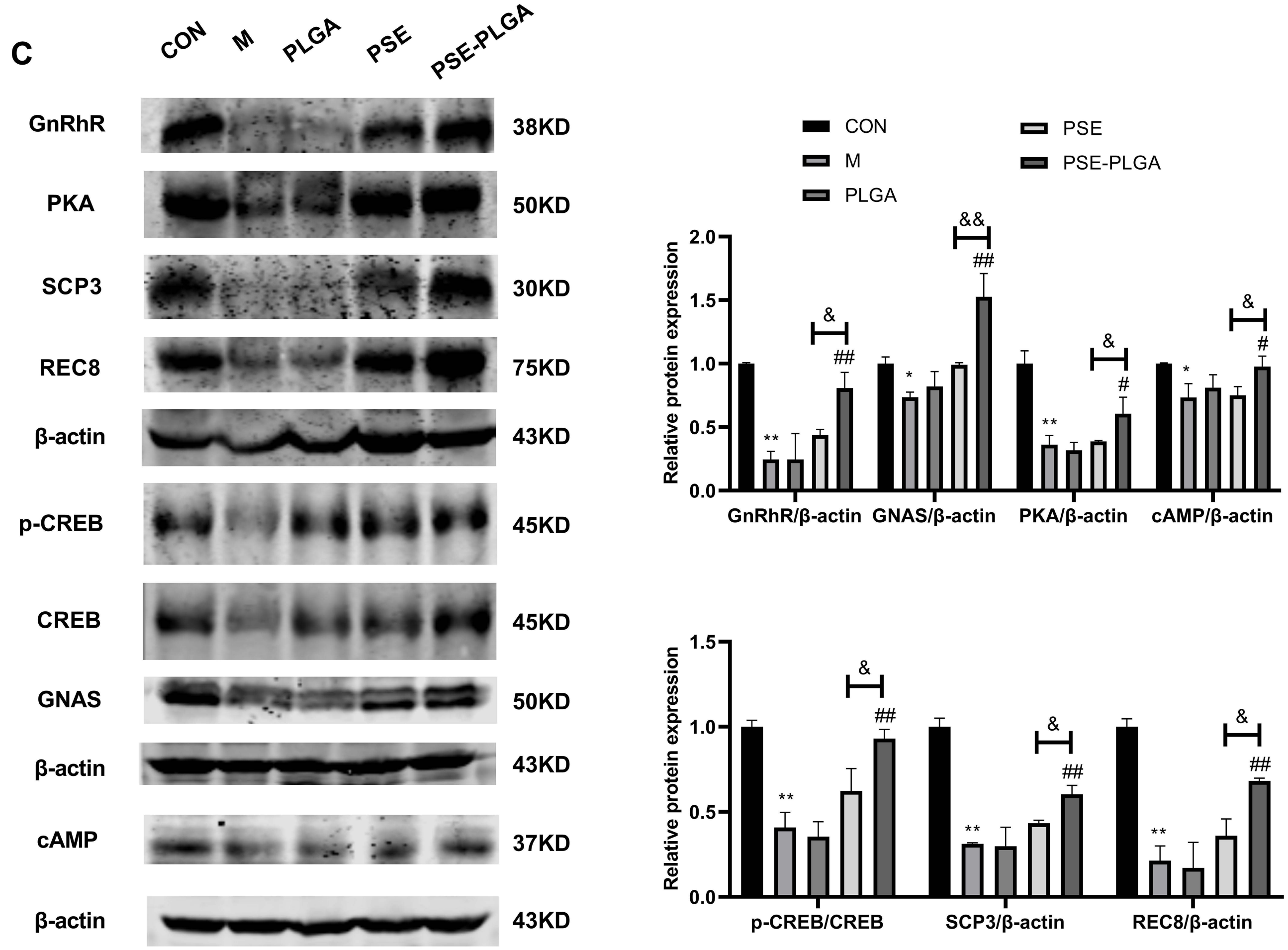

Figure 7 Continued.

application of PLGA-NPs significantly improved the effect of PSE. After preliminary determination of the role of PSE-NPs, we conducted in vivo experiments in mice.

Weight is a key indicator to evaluate the side-effects of drugs.[21,37] In vivo studies showed that PSE-NPs had no effect on the bodyweight of mice in the present study. Adriamycin could reduce sperm motility significantly and increase the number of dead sperm in mice. PSE-NPs treatment significantly increased the total number of sperm and sperm motility, and decreased the proportion of dead sperm. We calculated the apoptosis level of testis by flow cytometry. PSE and PSE-NPs could reduce the percent apoptosis of testicular cells and improve the level of living cells, while PSE-NPs had better effect. Generally, oxidative stress has been considered to be an initiating event of reproductive toxicity. It occurs when the production of potentially destructive reactive oxygen species (ROS) exceeds the body's own natural antioxidant defenses. Therefore, MDA as a marker of lipid peroxidation, accumulates, while SOD as a major scavenger of ROS is depleted.[38] Previous reports have linked testosterone reduction to the pro-apoptotic caspase 3 activity and apoptosis of the germ cell line.[24,39] TNFα mediates doxorubicin apoptosis via activation of caspase 3 and IL-1.[23,40] We also examined the activation of apoptotic pathways in the testes using BAX as the proapoptotic protein and Bcl-2 as the anti-apoptotic protein. ADM could give rise to obvious apoptosis and oxidative stress in GC-1 cells, up-regulated expression of apoptosis-related proteins (Bax, TNF-α, IL-1β, MDA, caspase 3) and downregulated expression of SOD and Bcl-2. PSE-NPs could significantly increase expression of antioxidant-associated proteins and reduce an excessive increase in expression of apoptosis-related proteins.

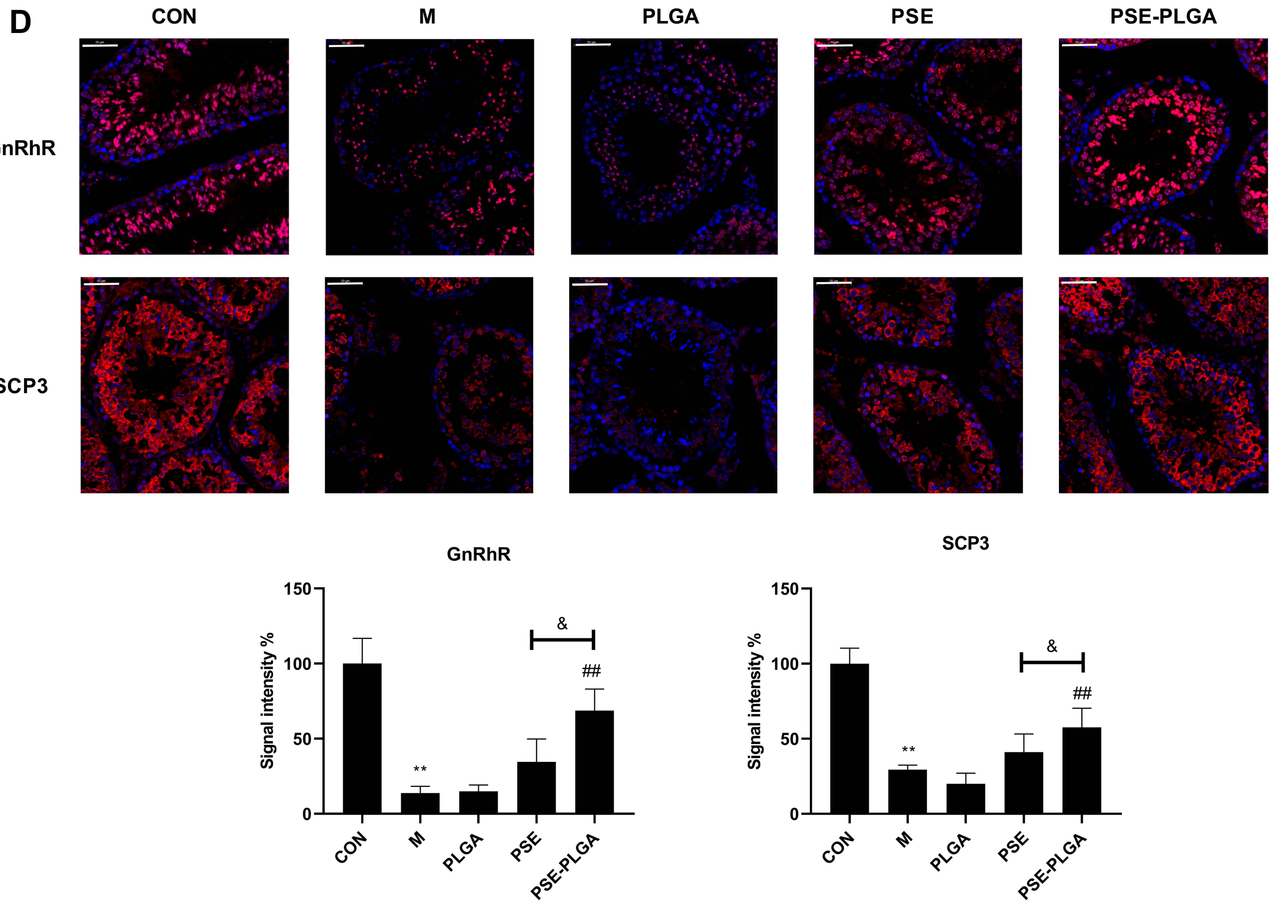

Figure 7 Effects of PSE-NPs on sex-hormone levels, GnRh signaling pathway-related proteins in testes, and indices of meiosis in mice: (**A**) Levels of GnRh, LH and testosterone in the serum of mice in each group. (**B**) mRNA expression of GnRh signaling pathway-related proteins and meiosis-associated genes in the testicular tissue of mice in each group was measured by RT-qPCR. (**C**) Protein expression of GnRh signaling pathway and meiosis-associated proteins in the testicular tissue of mice in each group was measured by western blotting. (**D**) The protein expression of GnRhR and SCP3 in the testicular tissue of mice in each group was measured by Immunofluorescence, scale bar 50 µm.
Notes: Data are the mean ± SD (n = 6). **P* < 0.05 and ***P* < 0.01 vs the CON group. #*P* < 0.05 and ##*P* < 0.01 vs the Model group. &*P* < 0.05 and &&*P* < 0.01 vs the PSE group.
Abbreviations: CON, Control group; M, Model group with 30 mg/kg adriamycin, i.p.; PSE, 1.4 mg/kg PSE, i.v.; PLGA, 53.8 mg/kg PLGAs, i.v.; PSE-PLGA, 53.8 mg/kg PSE-PLGAs, i.v.; GnRh, gonadotropin-releasing hormone; LH, luteinizing hormone; GnRHR, gonadotropin-releasing hormone receptor; LHR, luteinising hormone receptor; AR, androgen receptor; GNAS, guanine nucleotide-binding proteins; ADCY1, adenylate cyclase type 1; PKA, protein kinase A; DAZ1, deleted in azoospermia protein 1; DDX4, Dead box polypeptide 4; STAR, StAR-related lipid transfer protein 8; SCP3, synaptonemal complex protein 3; REC8, meiotic recombination protein; SMC1B, structural maintenance of chromosomes protein 1B; Miwi, murine piwi gene; cAMP, Cyclic Adenosine monophosphate.

Studies have shown that problems in male reproductive health are often accompanied by dysregulation of sex-hormone levels. Hormones play a key part in development of the reproductive system.[41,42] Regulation of GnRh secretion in the body can enhance sexual function and maintain sperm quality and gonadal function.[43,44] GnRh is associated with sperm generation and smooth progression of meiosis.[45,46] Therefore, we measured the levels of GnRh, LH and testosterone. We found that PSE-NPs could increase the level of GnRh, LH and testosterone significantly. It also could significantly increase the mRNA levels of LHR and AR in testes. Studies have shown that expression of the proteins associated with the cAMP signaling pathway is inhibited significantly in testicular injury, including cAMP, PKA, CREB, and p-CREB.[47,48] ADCY1 is a member of the ADCY superfamily and is responsible for catalyzing ATP to cAMP.[49] If testicular injury occurs, GnRhR expression decreases significantly,[50] which can lead to inhibition of the GnRhR signaling pathway. Our results showed that adriamycin could inhibit the GnRhR signaling pathway significantly, PSE could up-regulate GnRH pathway with certain extent. Compared with PSE group, we found that PSE-NPs significantly increased the level of the GnRh/cAMP signaling pathway according to western blotting, RT-qPCR and immunofluorescence studies, as well as expression of its downstream signaling proteins, such as GnRhR, GNAS, ADCY1, cAMP, PKA and p-CREB/CREB.

The GnRhR signaling pathway is related to meiosis. If the GnRhR signaling pathway is inhibited, then expression of genes related to meiosis is also inhibited, thereby which reduces sperm production.[45,51] SCP3 is a key factor in meiosis, expressed mainly in primary spermatocytes.[52] SCP3-knockout homozygous male mice are infertile, with a significant decrease in the Testes Index and many apoptotic sperm cells.[53] REC8 protein enables the separation of homologous chromosomes during the meiosis of sperm cells, avoids the premature separation of sister chromatids, and guarantees the formation of mature haploid sperm.[54] We measured the levels of proteins associated with meiosis of sperm, SCP3 and REC8, and related genes, including *DAZ1, DDX4, CYCLIN-1, STAR, SMC1B* and *Miwi*.[55–60] Our results showed that adriamycin significantly inhibited the ability of mice to carry out meiosis of sperm, PSE could promote expression of the proteins and genes related to meiosis. Compared with PSE group, PSE-NPs significantly promoted expression of the proteins and genes related to meiosis. The in vivo and in vitro results are consistent, further demonstrating that the PSE alleviate adriamycin-induced reproductive toxicity through the GnRhR signaling pathway and the effect can be enhanced after encapsulated with PLGA-NPs.

PSE-NPs not only show a helpful impact, but also appear to have no obvious biological toxicity, which show that they have colossal potential as a candidate treatment for reducing adriamycin-induced reproductive toxicity. The results of this study indicate that PSE-NPs incorporate a certain defensive impact on adriamycin-induced reproductive toxicity, and its preliminary mechanism may be related to activation of the GnRhR signaling pathway, which promotes expression of meiosis-related factors. This study provides preliminary proof for the PSE-NPs' alleviation of adriamycin-induced reproductive toxicity. Be that as it may, further research is required to determine the underlying mechanism and bioactivity.

Conclusions

Our results suggest that PSE-NPs reduce adriamycin-induced reproductive toxicity. This action may be associated with activation of the GnRhR signaling pathway, which promotes expression of meiosis-related factors. The clinical application of PSE-NPs merits further research.

Acknowledgments

This work was supported by the National Key Research and Development Program (Major Project for Research of the Modernization of TCM; 2019YFC1708802), Henan Province High-Level Personnel Special Support ("ZhongYuan One Thousand People Plan"; Zhongyuan Leading Talent (ZYQR201810080)) and Key Scientific Research Projects of Colleges and Universities of Henan Province (21A360014).

Author Contributions

All authors made a significant contribution to the work reported, whether that is in the conception, study design, execution, acquisition of data, analysis and interpretation, or in all these areas; took part in drafting, revising or critically reviewing the article; gave final approval of the version to be published; have agreed on the journal to which the article has been submitted; and agree to be accountable for all aspects of the work.

Disclosure

The authors declare that they have no competing interests.

References

1. Levi M, Tzabari M, Savion N, Stemmer SM, Shalgi R, Ben-Aharon I. Dexrazoxane exacerbates doxorubicin-induced testicular toxicity. *Reproduction*. 2015;150(4):357–366. doi:10.1530/rep-15-0129
2. Rendtorff R, Hohmann C, Reinmuth S, et al. Hormone and sperm analyses after chemo- and radiotherapy in childhood and adolescence. *Klin Padiatr*. 2010;222(3):145–149. doi:10.1055/s-0030-1249658
3. Ibrahim RYM, Mansour SM, Elkady WM. Phytochemical profile and protective effect of Ocimum basilicum aqueous extract in doxorubicin/irradiation-induced testicular injury. *J Pharm Pharmacol*. 2020;72(1):101–110. doi:10.1111/jphp.13175

4. Robertson J, Barr R, Shulman LN, Forte GB, Magrini N. Essential Medicines for cancer: WHO recommendations and national priorities. *Bull World Health Organ*. 2016;94(10):735–742. doi:10.2471/blt.15.163998
5. Herrmann J, Lerman A, Sandhu NP, Villarraga HR, Mulvagh SL, Kohli M. Evaluation and management of patients with heart disease and cancer: cardio-oncology. *Mayo Clin Proc*. 2014;89(9):1287–1306. doi:10.1016/j.mayocp.2014.05.013
6. Rahman AM, Yusuf SW, Ewer MS. Anthracycline-induced cardiotoxicity and the cardiac-sparing effect of liposomal formulation. *Int J Nanomedicine*. 2007;2(4):567–583.
7. Hou M, Chrysis D, Nurmio M, et al. Doxorubicin induces apoptosis in germ line stem cells in the immature rat testis and amifostine cannot protect against this cytotoxicity. *Cancer Res*. 2005;65(21):9999–10005. doi:10.1158/0008-5472.Can-05-2004
8. Mykoniatis I, Renterghem KV, Sokolakis I. How can we preserve sexual function after ablative surgery for benign prostatic hyperplasia? *Curr Drug Targets*. 2021;22(1):4–13. doi:10.2174/1389450121666200925143916
9. Shoshany O, Abhyankar N, Elyaguov J, Niederberger C. Efficacy of treatment with pseudoephedrine in men with retrograde ejaculation. *Andrology*. 2017;5(4):744–748. doi:10.1111/andr.12361
10. Ren M, Song S, Liang D, Hou W, Tan X, Luo J. Comparative tissue distribution and excretion study of alkaloids from herba ephedrae-radix aconiti lateralis extracts in rats. *J Pharm Biomed Anal*. 2017;134:137–142. doi:10.1016/j.jpba.2016.11.027
11. Xu R, Wang J, Xu J, et al. Rhynchophylline loaded-mPEG-PLGA nanoparticles coated with tween-80 for preliminary study in Alzheimer's Disease. *Int J Nanomedicine*. 2020;15:1149–1160. doi:10.2147/ijn.s236922
12. Li P, Bukhari SNA, Khan T, et al. Apigenin-loaded solid lipid nanoparticle attenuates diabetic nephropathy induced by streptozotocin nicotinamide through Nrf2/HO-1/NF-kB signalling pathway. *Int J Nanomedicine*. 2020;15:9115–9124. doi:10.2147/ijn.s256494
13. Liu CJ, Yao L, Hu YM, Zhao BT. Effect of quercetin-loaded mesoporous silica nanoparticles on myocardial ischemia-reperfusion injury in rats and its mechanism. *Int J Nanomedicine*. 2021;16:741–752. doi:10.2147/ijn.s277377
14. Iacovelli J, Rowe GC, Khadka A, et al. PGC-1α induces human RPE oxidative metabolism and antioxidant capacity. *Invest Ophthalmol Vis Sci*. 2016;57(3):1038–1051. doi:10.1167/iovs.15-17758
15. Gao L, Yuan P, Zhang Q, et al. Taxifolin improves disorders of glucose metabolism and water-salt metabolism in kidney via PI3K/AKT signaling pathway in metabolic syndrome rats. *Life Sci*. 2020;263:118713. doi:10.1016/j.lfs.2020.118713
16. Fedato RP, Maistro EL. Absence of genotoxic effects of the coumarin derivative 4-methylesculetin in vivo and its potential chemoprevention against doxorubicin-induced DNA damage. *J Appl Toxicol*. 2014;34(1):33–39. doi:10.1002/jat.2823
17. Fouad AA, Refaie MMM, Abdelghany MI. Naringenin palliates cisplatin and doxorubicin gonadal toxicity in male rats. *Toxicol Mech Methods*. 2019;29(1):67–73. doi:10.1080/15376516.2018.1512180
18. Belhan S, Özkaraca M, Özdek U, Kömüroğlu AU. Protective role of chrysin on doxorubicin-induced oxidative stress and DNA damage in rat testes. *Andrologia*. 2020;52(9):e13747. doi:10.1111/and.13747
19. Hou Y, Yuan P, Fu Y, et al. Duzhong butiansu prescription improves heat stress-induced spermatogenic dysfunction by regulating sperm formation and heat stress pathway. *Evid Based Complement Alternat Med*. 2020;2020:6723204. doi:10.1155/2020/6723204
20. Al-Megrin WA, El-Khadragy MF, Hussein MH, et al. Green coffea arabica extract ameliorates testicular injury in high-fat diet/streptozotocin-induced diabetes in rats. *J Diabetes Res*. 2020;2020:6762709. doi:10.1155/2020/6762709
21. Yuan L, Li Q, Bai D, et al. La(2)O(3) nanoparticles induce reproductive toxicity mediated by the Nrf-2/ARE signaling pathway in Kunming mice. *Int J Nanomedicine*. 2020;15:3415–3431. doi:10.2147/ijn.S230949
22. Fu Y, Yuan PP, Cao YG, et al. Geniposide in Gardenia jasminoides var. radicans Makino modulates blood pressure via inhibiting WNK pathway mediated by the estrogen receptors. *J Pharm Pharmacol*. 2020;72(12):1956–1969. doi:10.1111/jphp.13361
23. Yang CC, Chen YT, Chen CH, Chiang JY, Zhen YY, Yip HK. Assessment of doxorubicin-induced mouse testicular damage by the novel second-harmonic generation microscopy. *Am J Transl Res*. 2017;9(12):5275–5288.
24. Smart E, Lopes F, Rice S, et al. Chemotherapy drugs cyclophosphamide, cisplatin and doxorubicin induce germ cell loss in an in vitro model of the prepubertal testis. *Sci Rep*. 2018;8(1):1773. doi:10.1038/s41598-018-19761-9
25. Tillem SM, Mellinger BC. Azoospermia due to aperistalsis of the vas deferens: successful treatment with pseudoephedrine. *Urology*. 1999;53(2):417–419. doi:10.1016/s0090-4295(98)00339-2
26. Das S, Neal CJ, Ortiz J, Seal S. Engineered nanoceria cytoprotection in vivo: mitigation of reactive oxygen species and double-stranded DNA breakage due to radiation exposure. *Nanoscale*. 2018;10(45):21069–21075. doi:10.1039/c8nr04640a
27. El-Maddawy ZK, Abd El Naby WSH. Protective effects of zinc oxide nanoparticles against doxorubicin induced testicular toxicity and DNA damage in male rats. *Toxicol Res (Camb)*. 2019;8(5):654–662. doi:10.1039/c9tx00052f
28. Schnieders J, Gbureck U, Thull R, Kissel T. Controlled release of gentamicin from calcium phosphate-poly(lactic acid-co-glycolic acid) composite bone cement. *Biomaterials*. 2006;27(23):4239–4249. doi:10.1016/j.biomaterials.2006.03.032
29. Kim IS, Lee SK, Park YM, et al. Physicochemical characterization of poly(L-lactic acid) and poly(D,L-lactide-co-glycolide) nanoparticles with polyethylenimine as gene delivery carrier. *Int J Pharm*. 2005;298(1):255–262. doi:10.1016/j.ijpharm.2005.04.017
30. Kakizawa Y, Nishio R, Hirano T, et al. Controlled release of protein drugs from newly developed amphiphilic polymer-based microparticles composed of nanoparticles. *J Control Release*. 2010;142(1):8–13. doi:10.1016/j.jconrel.2009.09.024
31. Khalil NM, Do Nascimento TC, Casa DM. Pharmacokinetics of curcumin-loaded PLGA and PLGA-PEG blend nanoparticles after oral administration in rats. *Colloids Surf B Biointerfaces*. 2013;101:353–360. doi:10.1016/j.colsurfb.2012.06.024
32. Zheng Z, Bian Y, Zhang Y, Ren G, Li G. Metformin activates AMPK/SIRT1/NF-κB pathway and induces mitochondrial dysfunction to drive caspase3/GSDME-mediated cancer cell pyroptosis. *Cell Cycle*. 2020;19(10):1089–1104. doi:10.1080/15384101.2020.1743911
33. Alotaibi MF, Al-Joufi F, Abou Seif HS, et al. Umbelliferone inhibits spermatogenic defects and testicular injury in lead-intoxicated rats by suppressing oxidative stress and inflammation, and improving Nrf2/HO-1 signaling. *Drug Des Devel Ther*. 2020;14:4003–4019. doi:10.2147/dddt.s265636
34. Pandey A, Yadav SK, Vishvkarma R, et al. The dynamics of gene expression during and post meiosis sets the sperm agenda. *Mol Reprod Dev*. 2019;86(12):1921–1939. doi:10.1002/mrd.23278
35. Meneses MJ, Bernardino RL, Sá R, et al. Pioglitazone increases the glycolytic efficiency of human Sertoli cells with possible implications for spermatogenesis. *Int J Biochem Cell Biol*. 2016;79:52–60. doi:10.1016/j.biocel.2016.08.011

36. Hsiao CH, Ji AT, Chang CC, Chien MH, Lee LM, Ho JH. Mesenchymal stem cells restore the sperm motility from testicular torsion-detorsion injury by regulation of glucose metabolism in sperm. *Stem Cell Res Ther*. 2019;10(1):270. doi:10.1186/s13287-019-1351-5
37. Khorsandi L, Orazizadeh M, Moradi-Gharibvand N, Hemadi M, Mansouri E. Beneficial effects of quercetin on titanium dioxide nanoparticles induced spermatogenesis defects in mice. *Environ Sci Pollut Res Int*. 2017;24(6):5595–5606. doi:10.1007/s11356-016-8325-2
38. Hasgul R, Uysal S, Haltas H, et al. Protective effects of Ankaferd blood stopper on aspirin-induced oxidative mucosal damage in a rat model of gastric injury. *Toxicol Ind Health*. 2014;30(10):888–895. doi:10.1177/0748233712466134
39. Kim JM, Ghosh SR, Weil AC, Zirkin BR. Caspase-3 and caspase-activated deoxyribonuclease are associated with testicular germ cell apoptosis resulting from reduced intratesticular testosterone. *Endocrinology*. 2001;142(9):3809–3816. doi:10.1210/endo.142.9.8375
40. Zhao L, Zhang B. Doxorubicin induces cardiotoxicity through upregulation of death receptors mediated apoptosis in cardiomyocytes. *Sci Rep*. 2017;7:44735. doi:10.1038/srep44735
41. Zhou L, Han L, Liu M, Lu J, Pan S. Impact of metabolic syndrome on sex hormones and reproductive function: a meta-analysis of 2923 cases and 14062 controls. *Aging*. 2020;13(2):1962–1971. doi:10.18632/aging.202160
42. Maggi R, Cariboni AM, Marelli MM, et al. GnRH and GnRH receptors in the pathophysiology of the human female reproductive system. *Hum Reprod Update*. 2016;22(3):358–381. doi:10.1093/humupd/dmv059
43. Luo J, Yang Y, Zhang T, et al. Nasal delivery of nerve growth factor rescue hypogonadism by up-regulating GnRH and testosterone in aging male mice. *EBioMedicine*. 2018;35:295–306. doi:10.1016/j.ebiom.2018.08.021
44. Chianese R, Cobellis G, Chioccarelli T, et al. Kisspeptins, estrogens and male fertility. *Curr Med Chem*. 2016;23(36):4070–4091. doi:10.2174/0929867323666160902155434
45. Yang W, Xu Y, Pan H, et al. Chronic exposure to diesel exhaust particulate matter impairs meiotic progression during spermatogenesis in a mouse model. *Ecotoxicol Environ Saf*. 2020;202:110881. doi:10.1016/j.ecoenv.2020.110881
46. Wang Y, Li Y, Chen Q, Liu Z. Diethylstilbestrol impaired oogenesis of yellow catfish juveniles through disrupting hypothalamic-pituitary-gonadal axis and germ cell development. *J Appl Toxicol*. 2018;38(3):308–317. doi:10.1002/jat.3529
47. Zhou Y, Ji J, Zhuang J, Wang L, Hong F. Nanoparticulate TiO_2 induced suppression of spermatogenesis is involved in regulatory dysfunction of the cAMP-CREB/CREM signaling pathway in mice. *J Biomed Nanotechnol*. 2019;15(3):571–580. doi:10.1166/jbn.2019.2704
48. Zhang Y, Li G, Zhong Y, et al. 1,2-Dichloroethane induces reproductive toxicity mediated by the CREM/CREB signaling pathway in male NIH Swiss mice. *Toxicol Sci*. 2017;160(2):299–314. doi:10.1093/toxsci/kfx182
49. Zou T, Liu J, She L, et al. A perspective profile of ADCY1 in cAMP signaling with drug-resistance in lung cancer. *J Cancer*. 2019;10(27):6848–6857. doi:10.7150/jca.36614
50. Cui Y, Liu J, Zhu Y, et al. Effects of sevoflurane on reproductive function of male rats and its main mechanism of action. *Inhal Toxicol*. 2019;31(11–12):392–398. doi:10.1080/08958378.2019.1698677
51. Arisha AH, Moustafa A. Potential inhibitory effect of swimming exercise on the Kisspeptin-GnRH signaling pathway in male rats. *Theriogenology*. 2019;133:87–96. doi:10.1016/j.theriogenology.2019.04.035
52. Qian C, Meng Q, Lu J, Zhang L, Li H, Huang B. Human amnion mesenchymal stem cells restore spermatogenesis in mice with busulfan-induced testis toxicity by inhibiting apoptosis and oxidative stress. *Stem Cell Res Ther*. 2020;11(1):290. doi:10.1186/s13287-020-01803-7
53. Yuan L, Liu JG, Zhao J, Brundell E, Daneholt B, Höög C. The murine SCP3 gene is required for synaptonemal complex assembly, chromosome synapsis, and male fertility. *Mol Cell*. 2000;5(1):73–83. doi:10.1016/s1097-2765(00)80404-9
54. Wassmann K. Sister chromatid segregation in meiosis II: deprotection through phosphorylation. *Cell Cycle*. 2013;12(9):1352–1359. doi:10.4161/cc.24600
55. Li Q, Qiao D, Song NH. Association of DAZ1/DAZ2 deletion with spermatogenic impairment and male infertility in the South Chinese population. *World J Urol*. 2013;31(6):1403–1409. doi:10.1007/s00345-013-1058-7
56. Yang Y, Xiao C, Zhang S, Zhoucun A, Li X, Zhang S. Preliminary study of the relationship between DAZ gene copy deletions and spermatogenic impairment in Chinese men. *Fertil Steril*. 2006;85(4):1061–1063. doi:10.1016/j.fertnstert.2005.09.025
57. Guo FZ, Zhang LS, Wei JL, et al. Endosulfan inhibiting the meiosis process via depressing expressions of regulatory factors and causing cell cycle arrest in spermatogenic cells. *Environ Sci Pollut Res Int*. 2016;23(20):20506–20516. doi:10.1007/s11356-016-7195-y
58. Shahin NN, El-Nabarawy NA, Gouda AS, Mégarbane B. The protective role of spermine against male reproductive aberrations induced by exposure to electromagnetic field - An experimental investigation in the rat. *Toxicol Appl Pharmacol*. 2019;370:117–130. doi:10.1016/j.taap.2019.03.009
59. Esfandiari F, Ashtiani MK, Sharifi-Tabar M, et al. Microparticle-mediated delivery of BMP4 for generation of meiosis-competent germ cells from embryonic stem cells. *Macromol Biosci*. 2017;17(3):1600284. doi:10.1002/mabi.201600284
60. Hsieh CL, Xia J, Lin H. MIWI prevents aneuploidy during meiosis by cleaving excess satellite RNA. *EMBO J*. 2020;39(16):e103614. doi:10.15252/embj.2019103614